

# Bulk-sensitive photoemission spectroscopy of $A_2FeMoO_6$ double perovskites (A=Sr, Ba)

J. -S. Kang<sup>1</sup>, J. H. Kim<sup>1</sup>, A. Sekiyama<sup>2</sup>, S. Kasai<sup>2</sup>, S. Suga<sup>2</sup>, S. W. Han<sup>3</sup>, K. H. Kim<sup>3</sup>, T. Muro<sup>4</sup>, Y. Saitoh<sup>5</sup>, C. Hwang<sup>6</sup>, C. G. Olson<sup>7</sup>, B. J. Park<sup>8</sup>, B. W. Lee<sup>8</sup>, J. H. Shim<sup>9</sup>, J. H. Park<sup>9</sup>, and B. I. Min<sup>9</sup>

<sup>1</sup>*Department of Physics, The Catholic University of Korea, Puchon 420-743, Korea*

<sup>2</sup>*Department of Material Physics, Graduate School of Engineering Science, Osaka University, Osaka 560-8531, Japan*

<sup>3</sup>*Department of Physics, Gyeongsang National University, Chinju 660-701, Korea*

<sup>4</sup>*Department of Synchrotron Radiation Research, Japan Atomic Energy Research Institute, SPring-8, Hyogo 679-5198, Japan*

<sup>5</sup>*Department of Synchrotron Radiation Research, Kansai Research Establishment, Japan Atomic Energy Research Institute, SPring-8, Hyogo 679-5198, Japan*

<sup>6</sup>*Korea Research Institute of Standards and Science, Taejeon 305-600, Korea*

<sup>7</sup>*Ames Laboratory, Iowa State University, Ames, Iowa 50011, U.S.A.*

<sup>8</sup>*Department of Physics, Hankuk University of Foreign Studies, Yongin, Kyungki 449-791, Korea*

<sup>9</sup>*Department of Physics, Pohang University of Science and Technology, Pohang 790-784, Korea*

(November 1, 2018)

Electronic structures of  $Sr_2FeMoO_6$  (SFMO) and  $Ba_2FeMoO_6$  (BFMO) double perovskites have been investigated using the  $Fe\ 2p \rightarrow 3d$  resonant photoemission spectroscopy (PES) and the Cooper minimum in the  $Mo\ 4d$  photoionization cross section. The states close to the Fermi level are found to have strongly mixed  $Mo-Fe\ t_{2g}$  character, suggesting that the Fe valence is far from pure  $3+$ . The  $Fe\ 2p_{3/2}$  XAS spectra indicate the mixed-valent  $Fe^{3+}-Fe^{2+}$  configurations, and the larger  $Fe^{2+}$  component for BFMO than for SFMO, suggesting a kind of double exchange interaction. The valence-band PES spectra reveal good agreement with the  $LSDA+U$  calculation.

PACS numbers: 79.60.-i, 75.70.Pa, 71.30.+h

Room-temperature magnetoresistance (MR) has been recently observed in the double-perovskite oxides of  $A_2BB'MoO_6$  (A=Sr, Ba; B=Fe, B'=Mo) with very high magnetic transition temperatures  $T_C$  ( $\simeq 330 - 450$  K) [1–3]. A fundamental question in the double perovskites is the origin of the high  $T_C$  ferrimagnetism and the low field MR. Magnetization data for  $Sr_2FeMoO_6$  (SFMO) indicate ferrimagnetic coupling between  $Fe^{3+}$  and  $Mo^{5+}$  ions [4], and the MR was interpreted as due to inter-grain tunneling with the half-metallic electronic structure [1,5,6]. Neutron diffraction and Mössbauer spectroscopy on  $A_2FeMoO_6$  (AFMO) indicated an Fe moment of  $4.0 \sim 4.1\ \mu_B$  but rather small localized moment on Mo,  $-0.2 \sim -0.5\ \mu_B$  [2,7,8]. The ferrimagnetic coupling between  $Fe^{3+}$  and  $Mo^{5+}$  can be understood in terms of the superexchange through the Fe-O-Mo  $\pi$ -bonding. The superexchange model, however, is not compatible with the metallic nature of SFMO and  $Ba_2FeMoO_6$  (BFMO). Further, the valence states of Fe and Mo ions are still controversial; some works are interpreted as the  $Fe^{3+}$  [1,9], while other works favor the mixed valence of  $Fe^{3+}-Fe^{2+}$  [7,10,11].

Photoemission spectroscopy (PES) can provide direct information on the electronic structures of the double perovskites, but no valence-band PES study on SFMO has been reported so far [12,13]. In this paper, we report the first bulk-sensitive high-resolution valence-band PES study for SFMO and BFMO, including resonant photoemission spectroscopy (RPES) near the  $Fe\ 2p$  absorption edge and the O  $1s$  and  $Fe\ 2p$  X-ray absorption spectroscopy (XAS) measurements.

Polycrystalline SFMO and BFMO samples were pre-

pared by the standard solid-state reaction method [12]. The measured saturation magnetic moments are larger than  $3.8\ \mu_B$  (BFMO) and  $3.4\ \mu_B$  (SFMO) per formula unit (f.u.), reflecting the well ordered Fe and Mo ions at B and B' sites. High-resolution  $Fe\ 2p \rightarrow 3d$  RPES experiments were performed at the BL25SU of SPring-8. [14]. Samples were fractured and measured in vacuum with a base pressure better than  $3 \times 10^{-10}$  Torr at  $T \lesssim 20$  K. The Fermi level  $E_F$  of the system was determined from the valence band spectrum of a scraped Pd sample. The total instrumental resolution [FWHM : full width at half maximum] was about 130 meV at  $h\nu \sim 700$  eV. All the spectra were normalized to the photon flux estimated from the mirror current. Low energy PES experiments were carried out at the Ames/Montana beamline at the Synchrotron Radiation Center (SRC) [12].

Figure 1 shows the RPES valence-band spectra of SFMO and BFMO near the  $Fe\ 2p_{3/2}$  absorption edge. The top panels show the measured  $Fe\ 2p_{3/2}$  XAS spectra (left) and the calculated XAS spectra (right). The arrows in the XAS spectra represent  $h\nu$ 's where the spectra are obtained. For both SFMO and BFMO, the features near  $E_F$  ( $\sim -0.3$  eV), at  $\sim -1.5$  eV, at  $-3$  eV, and  $-4$  eV in the valence-band spectra are enhanced greatly across the  $Fe\ 2p$  absorption edge, indicating that these states have large  $Fe\ 3d$  character. As to the resonating behavior, the  $Fe\ 3d$ -derived states at  $-0.3$  eV and at  $-1.5$  eV are due to the  $t_{2g}^x \downarrow$  and  $e_g^2 \uparrow$  states, respectively ( $0 < x \lesssim 1$ ) [12]. These RPES measurements reveal that the high binding energy (BE) features ( $-3 \sim -8$  eV) also have the substantially large  $Fe\ 3d$  electron character, which is strongly hybridized with the O  $2p$  electrons. In the

above  $h\nu$  region, however, the features for  $E \lesssim -5$  eV are obscured by the overlapping broad Fe LMM Auger emission, which is evident as the non-flat slope for  $E \lesssim -8$  eV for  $h\nu \gtrsim 708$  eV.

Our Fe  $2p_{3/2}$  XAS spectrum for SFMO is basically similar to those of previous reports [9,15]. But the low- $h\nu$  shoulder around  $h\nu \sim 707$  eV, which is present in our XAS spectra of both SFMO and BFMO, is missing in the existing data, which is due to the better resolution ( $\sim 100$  meV) employed in our XAS spectra. It is evident that the relative intensities between the two peaks of the  $2p_{3/2}$  absorption maxima ( $h\nu \approx 708$  eV, 710 eV) are reversed in SFMO and BFMO; namely a stronger peak is located at a higher  $h\nu$  for SFMO but at a lower  $h\nu$  for BFMO. We believe that this difference is intrinsic since both samples showed a clean single peak in the O  $1s$  core-level spectrum, and essentially the same XAS spectrum was reproduced for BFMO with different fractures. It has been known that the  $2p_{3/2}$  absorption edge of  $\text{Fe}^{2+}$  ions in the octahedral symmetry exhibits a main peak at a lower  $h\nu$  than that of  $\text{Fe}^{3+}$  ions [16,17]. Thus the difference in the Fe  $2p_{3/2}$  XAS spectra between SFMO and BFMO suggests that Fe ions in BFMO have a larger  $2+$  component than in SFMO. One possible reason for such a difference might be the different oxygen relaxation between Fe and Mo due to different ion radii of Ba and Sr ions. Indeed the structural data provides that the relative Fe-O bond length is smaller in SFMO to have higher Fe valence state, than in BFMO [8,18].

In order to estimate the Fe valences of SFMO and BFMO in the ground states, we have analyzed the XAS spectra of SFMO and BFMO within the configuration interaction cluster model where the effects of the multiplet interaction, the crystal field, and the hybridization with the O  $p$  ligands are included [19,20]. The calculated XAS spectra are shown in the top-right panels, where dotted lines, grey lines, and solid lines denote the  $\text{Fe}^{2+}$  and  $\text{Fe}^{3+}$  component, and their sum, respectively. This analysis shows that the ground states of both SFMO and BFMO have the  $\text{Fe}^{3+} - \text{Fe}^{2+}$  mixed states, but that BFMO has the larger  $\text{Fe}^{2+}$  component. If we use the  $\text{Fe}^{3+}$  component only ( $d^5$  and  $d^6\bar{\underline{L}}^1$ ,  $\bar{\underline{L}}$ : a ligand hole), the experimental features of the reversed XAS lineshape for BFMO and the low- $h\nu$  shoulders ( $h\nu \sim 707$  eV) cannot be reproduced. This analysis implies that the ground states of SFMO and BFMO are strongly mixed-valent with the  $\text{Fe}^{3+} - \text{Mo}^{5+}$  and  $\text{Fe}^{2+} - \text{Mo}^{6+}$  configurations.

Figure 2 compares the valence-band spectra of SFMO and BFMO for a wide  $h\nu$  range ( $22 \text{ eV} \leq h\nu \lesssim 700 \text{ eV}$ ). The top two spectra are the differences between the on-resonance ( $h\nu \approx 708$  eV) and off-resonance spectra in the Fe  $2p \rightarrow 3d$  RPES, which can be considered as representing the Fe  $3d$  partial spectral weight (PSW) distributions. If one assumes  $\text{Fe}^{3+}$  ( $3d^5$ ),  $\text{Mo}^{5+}$  ( $4d^1$ ), and the filled O  $2p$  bands ( $2p^6$ ) in AFMO, then the cross-section ratio of Fe  $3d$  : Mo  $4d$  : O  $2p$  per unit cell is about  $\sim 4\%$  :  $\sim 5\%$  :  $\sim 91\%$  at  $h\nu \approx 20$  eV,  $\sim 25\%$  :  $\sim 0\%$  :  $\sim 75\%$  at  $h\nu \approx 90$  eV, and  $\sim 41\%$  :  $\sim 9\%$  :  $\sim 49\%$  at  $h\nu \approx 700$

eV according to an atomic photoionization cross-section calculation [21]. The  $h\nu = 22$  eV spectrum can be considered as the O  $2p$  PSW because of the dominant O  $2p$  emission at  $h\nu = 22$  eV. With increasing  $h\nu$ , the Fe  $3d$  and Mo  $4d$  emissions increase with respect to the O  $2p$  emission, except for the  $h\nu$  region corresponding to the Cooper minimum in the Mo  $4d$  cross section around  $h\nu \sim 90$  eV, and the Fe  $3d$  and O  $2p$  emissions become comparable at  $h\nu \approx 700$  eV. Consequently, the Mo  $4d$  emission is negligible at  $h\nu \sim 90$  eV, and becomes the largest in the Fe  $3d$  off-resonance spectrum ( $h\nu = 704$  eV). Thus the pronounced feature at  $E_F$  at  $h\nu = 704$  eV is due to the larger Mo  $4d$  contribution than at other  $h\nu$ 's, and may also represent the intrinsic feature in the bulk PES spectra [22].

The valence-band spectra of SFMO and BFMO share very common features. First, metallic Fermi edges are observed in both systems at  $T \sim 20$  K, which confirms the metallic behavior at low  $T$ . Secondly, several structures appear at similar energies, labeled as  $\alpha$  ( $-0.3$  eV),  $\beta$  ( $-1.5$  eV),  $\gamma$  ( $-3.5$  eV),  $\delta$  ( $-4$  eV), and  $\epsilon$  ( $\sim -8$  eV). Based on the finding in Fig. 1, the features of  $\alpha$ ,  $\beta$ ,  $\gamma$ ,  $\delta$  are identified to have large Fe  $3d$ -derived electron character. Note that the peak  $\alpha$  is much larger at  $h\nu = 704$  eV than at  $h\nu = 90$  eV (Cooper minimum), indicating that the peak  $\alpha$  has predominant Mo  $4d$  electron character. Therefore this figure provides experimental evidence that the peak  $\alpha$  has both Mo  $4d$  and Fe  $3d$  electron character, but with larger Mo  $4d$  character.

We now discuss the differences in the valence-band spectra between SFMO and BFMO. First, the  $\alpha$  peak at  $E_F$  for BFMO is weaker than that in SFMO with respect to the  $\epsilon$  peak, and secondly the band width of the O  $2p$ -Fe  $3d$  peak in BFMO is narrower than that in SFMO. The former difference suggests that the Mo  $4d$  electron occupancy in BFMO is lower than that in SFMO since  $\alpha$  has both Fe  $3d$  and Mo  $4d$  electron character but the intensity of the peak  $\alpha$  in the Fe  $3d$  PSW is the same for SFMO and BFMO. Accordingly, this finding indicates larger  $\text{Fe}^{2+} - \text{Mo}^{6+}$  character in BFMO than in SFMO, which is consistent with that of the Fe  $2p_{3/2}$  XAS spectra (Fig. 1). The difference in the bandwidth is in agreement with the LSDA+ $U$  ( $U$ : the Coulomb correlation parameter) calculations shown in Fig. 3, and reflects the larger Fe-O-Mo bond length in BFMO due to its larger lattice constant [18].

The left panel of Fig. 3 compares the  $h\nu = 704$  eV valence-band spectra (dots) to the weighted sum of the PLDOSs (projected local densities of states) of Fe  $3d$ , Mo  $4d$ , and O  $2p$  states (solid lines). The PLDOSs have been obtained from the LSDA+ $U$  calculation [12]. The parameters used in this calculation are  $U = 3.0$  eV and  $J = 0.97$  eV ( $J$ : the exchange correlation parameter) for Fe  $3d$  electrons. For the comparison to the valence-band spectra, the summed PLDOSs below  $E_F$  have been convoluted with a Gaussian function of 0.2 eV at FWHM to simulate the instrumental resolution. The right panel compares the O  $1s$  XAS spectra to the sum of the unoc-

cupied part of the Fe  $3d$ , Mo  $4d$ , O  $2p$ , and Sr (Ba)  $s/p$  PLDOSs. The O  $1s$  XAS spectrum provides a reasonable approximation for representing the unoccupied conduction bands since it reflects the transition from the O  $1s$  to the unoccupied O  $2p$  states hybridized to the other electronic states. The calculated integer total magnetic moments ( $4.0 \mu_B$  per f.u.) are consistent with the half-metallic nature of SFMO and BFMO.

In the valence-band spectra, the lowest energy peak of  $\alpha$  arises from the Mo  $t_{2g} \downarrow$  – Fe  $t_{2g} \downarrow$  hybridized states with the occupied bandwidth of  $\sim 1$  eV. The features of  $\beta$  and  $\gamma$  have mainly Fe  $e_g \uparrow$  and Fe  $t_{2g} \uparrow$  character, respectively. The high BE feature  $\epsilon$  originates from the Mo  $4d$ – Fe  $3d$ – O  $p$  hybridized bonding states. In the XAS spectra, the low energy peak  $\alpha'$  has mainly Mo  $t_{2g} \uparrow$  and Fe  $t_{2g} \downarrow$  character. The feature of  $\beta'$  originates from Fe  $e_g \downarrow$  states, and  $\gamma'$  from Mo  $e_g \uparrow\downarrow$  states. The weak feature  $\delta'$  is due to Mo  $t_{2g} \downarrow$  states. It is clearly shown that the LSDA+ $U$  calculations agree quite well with the valence-band spectra, in the peak positions and the band widths, and also explain the low energy features of the XAS spectra reasonably well. If we shift the O  $1s$  XAS spectra by referring to the LSDA+ $U$  calculations [12,23], the energy separations between the lowest energy peaks in the valence-band PES ( $\alpha$ ) and those in the O  $1s$  XAS ( $\alpha'$ ) spectra become about  $\sim 1$  eV. This value is comparable to, but slightly larger than the low energy peak observed in the optical conductivity spectrum for SFMO [6], which was ascribed to the Fe  $e_{2g} \uparrow \rightarrow$  Mo  $t_{2g} \uparrow$  interband transition. We, however, ascribe this energy separation to the energy difference between the occupied Mo  $t_{2g} \downarrow$  – Fe  $t_{2g} \downarrow$  hybridized state and the unoccupied Fe  $t_{2g} \downarrow$  state mixed with O  $p$ –Mo  $t_{2g}$  states.

We have found that the Fe  $t_{2g} \downarrow$  and Mo  $t_{2g} \downarrow$  bands are almost degenerate and so  $t_{2g}$  electrons become itinerant, suggesting that two degenerate valence states Fe $^{3+}$  – Mo $^{5+}$  and Fe $^{2+}$  – Mo $^{6+}$  would produce a type of double exchange (DE) interaction [24]. That is, hopping of itinerant  $t_{2g} \downarrow$  electrons between Fe and Mo sites yields a kinetic energy gain to induce ferrimagnetism between Fe and Mo spins and the half metallicity in SFMO and BFMO. Therefore Fe and Mo ions in SFMO and BFMO do not have definite valence states [10,11]. The difference from the case of CMR manganites is that the spins of itinerant carriers are opposite to the localized Fe spins ( $t_{2g}^3 \uparrow e_g^2 \uparrow$ ). Sarma *et al.* [13] and Fang *et al.* [25] have recently proposed alternative models to explain the magnetism in double perovskites. They regard the double perovskite system as a ferromagnet not a ferrimagnet. That is, originally nonmagnetic Mo  $t_{2g}$  electrons are antiferromagnetically polarized by the ferromagnetically ordered Fe $^{3+}$  spins through the hybridization between Fe  $3d$  and Mo  $4d$  states, thereby the resulting kinetic energy gain stabilizes the ferromagnetic state. In view of the role of kinetic energy optimization, this mechanism seems similar to the DE mechanism. However, using their models, it is hard to explain the ferrimagnetism observed in the insulating double perovskites such as Ca $_2$ FeReO $_6$

and Ba $_2$ BReO $_6$  ( $B$ =Mn, Co, Ni) which have one more  $d$  electron in the B' site [24].

Ferrimagnetism in the insulating double perovskites of A $_2$ BB'O $_6$  is better described in terms of the superexchange interaction through B-B'-O  $\pi$  orbitals. In the metallic SFMO and BFMO systems, the DE-like interaction becomes operative due to the degenerate Fe and Mo  $t_{2g} \downarrow$  states near  $E_F$ . In the DE mechanism, the magnetic transition temperature  $T_C$  is proportional to the hopping strength, i.e., the bandwidth of the itinerant  $t_{2g} \downarrow$  states [26]. The observed correlation between  $T_C$  and the estimated bandwidth in metallic double perovskites provides evidence for the operation of the DE-like interaction [18]. Noteworthy is that both the superexchange and the DE interactions induce the ferrimagnetism in double perovskites, differently from the case of CMR manganites in which two interactions are competitive. Further, the Jahn-Teller effect would be weaker in double perovskites due to relevant  $t_{2g}$  orbitals near  $E_F$ , as compared to  $e_g$  orbitals in manganites. Hence  $T_C$  can be high for SFMO and BFMO.

In conclusion, using the bulk-sensitive Fe  $2p \rightarrow 3d$  RPES and O  $1s$  XAS, the states close to  $E_F$  are found to be predominantly of Mo  $t_{2g} \downarrow$  and Fe  $t_{2g} \downarrow$  character, indicating that the Fe valence is far from pure 3+ ( $d^5$ ). The Fe  $2p_{3/2}$  XAS spectra shows that the ground states of both SFMO and BFMO consist of the strongly-mixed Fe $^{3+}$ –Fe $^{2+}$  configurations, and that BFMO has the larger Fe $^{2+}$  component. The measured valence-band spectra agree very well with the LSDA+ $U$  calculation, suggesting that the DE-like interaction is operative to produce the half metallicity and ferrimagnetism in SFMO and BFMO.

Acknowledgments— Helpful discussions with D.D. Sarma are greatly appreciated. This work was supported by the KOSEF through the CSCMR at SNU and the eSSC at POSTECH. PES experiments were performed at the SPring-8 (JASRI: 2000B0028-NS- $\eta$ p) and at the SRC (NSF: DMR-0084402).

- 
- [1] K.-I. Kobayashi, *et al.*, Nature (London) **395**, 677 (1998).
  - [2] R. P. Borges, *et al.*, J. Phys.: Condens. Matter **11**, L445 (1999).
  - [3] Y. Moritomo, *et al.*, Phys. Rev. B **61**, R7827 (2000).
  - [4] F. S. Galasso, F. C. Douglas, and R. J. Kasper, J. Chem. Phys. **44**, 1672 (1966).
  - [5] T. H. Kim, *et al.*, Appl. Phys. Lett. **74**, 1737 (1999).
  - [6] Y. Tomioka, *et al.*, Phys. Rev. B **61** 422 (2000).
  - [7] B. Garcia-Landa, *et al.*, Solid State Commun. **110**, 435 (1999).
  - [8] Y. Moritomo, *et al.*, Phys. Rev. B **62**, 14224 (2000).
  - [9] S. Ray, *et al.*, Phys. Rev. Lett. **87**, 097204 (2001).
  - [10] J. Linden, *et al.*, Appl. Phys. Lett. **76**, 2925 (2000).

- [11] O. Chmaissem, *et al.*, Phys. Rev. B **62**, 14197 (2000).  
 [12] J.-S. Kang, *et al.*, Phys. Rev. B **64**, 024429 (2001); J.-S. Kang, *et al.*, to appear in J. Phys. Soc. Japan (2002).  
 [13] D. D. Sarma, *et al.*, Phys. Rev. Lett. **85**, 2549 (2000) (Mo 3d core-level PES study).  
 [14] Y. Saitoh, *et al.*, Rev. Sci. Instrum. **71**, 3254 (2000).  
 [15] M. S. Moreno, *et al.*, Solid State Comm. **120**, 161 (2001).  
 [16] G. van der Laan and I. W. Kirkman, J. Phys.: Condens. Matter **4**, 4189 (1992).  
 [17] J. P. Crocombette, *et al.*, Phys. Rev. B **52**, 3143 (1995).  
 [18] C. Ritter, *et al.*, J. Phys.: Condens. Matter **12**, 8295 (2000).  
 [19] F. M. F. de Groot, J. Elec. Spectrosc. Relat. Phenom., **67**, 529 (1994).  
 [20] J. H. Shim and B. I. Min, to be published elsewhere.  
 [21] J.J. Yeh and I. Lindau, *At. Nucl. Data Tables* **32**, 1 (1985).  
 [22] A. Sekiyama, *et al.*, Nature (London) **403**, 398 (2000).  
 [23] The O 1s XAS spectra of SFMO and BFMO are shifted by  $-528.7$  eV and  $-528.5$  eV, respectively. There is uncertainty in choosing the zero positions in the XAS spectra.  
 [24] A. W. Sleight and J. F. Weiher, J. Phys. Chem. Solids, **33**, 679 (1972).  
 [25] Z. Fang, K. Terakura, and J. Kanamori, Phys. Rev. B **63** 180407 (2001).  
 [26] A. Chattopadhyay and A. J. Millis, Phys. Rev. B **64**, 024424 (2001).

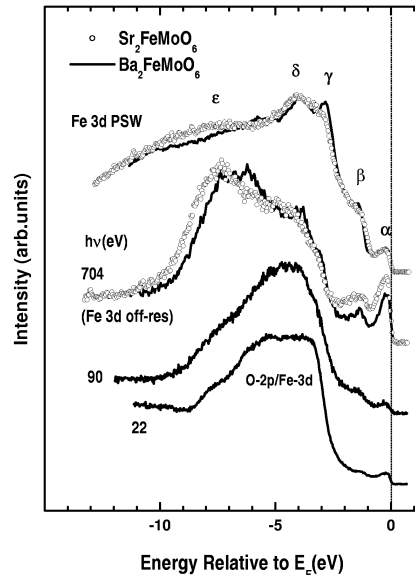


FIG. 2. Comparison of the valence-band spectra of SFMO (dots) and BFMO (solid lines) for a wide  $h\nu$  range.

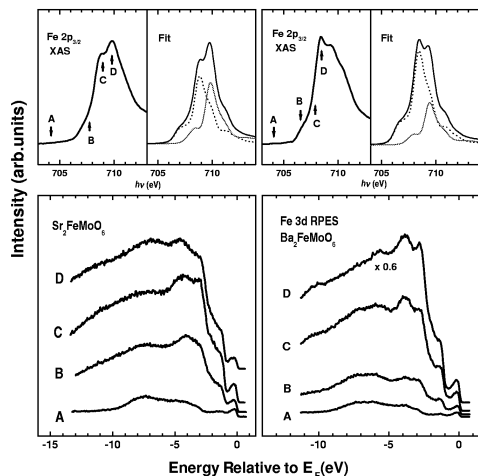


FIG. 1. Top: The measured Fe  $2p_{3/2}$  XAS spectra (left) and the fitting results (right) for SFMO and BFMO (see the text). Bottom: Valence-band spectra of SFMO and BFMO near the Fe  $2p \rightarrow 3d$  absorption edge.

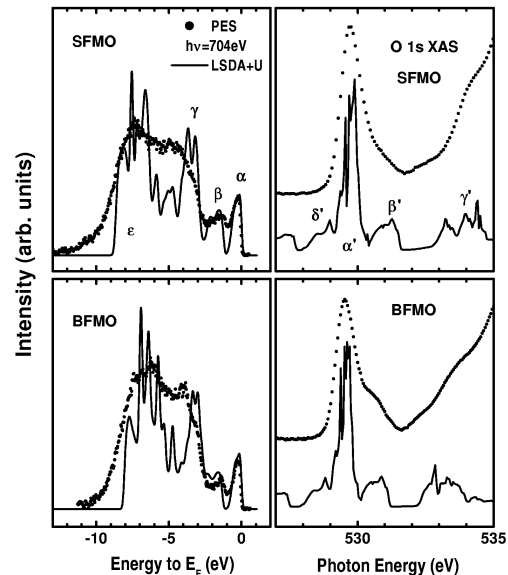


FIG. 3. Left: Comparison of the  $h\nu = 704$  eV valence-band spectra (dots) to the weighted sum of the PLDOSs (solid lines) obtained from the LSDA+ $U$  calculation. Right: Comparison of the O 1s XAS spectra to the sum of the Fe 3d, Mo 4d, O 2p, and Sr(Ba)  $s/p$  PLDOSs.